Monthly Notices
of the
ROYAL ASTRONOMICAL SOCIETY

MNRAS (2017) doi:10.1093/mnras/stx695

Radial variations of the volume and surface star formation laws in the Galaxy

Yoshiaki Sofue*

Institute of Astronomy, The University of Tokyo, Mitaka, Tokyo 181-0015, Japan

Accepted 2017 March 17. Received 2017 March 8; in original form 2016 November 26

ABSTRACT

Variation of the volume and surface Schmidt laws (star formation or SF law) with the galactocentric distance R was investigated using 3D distributions of H II regions, H I, and molecular (H_2) gases in the Milky Way. Both the power-law index and SF coefficient were found to vary with R. The index is flatter in the inner disc than in the outer Galaxy, and the coefficient is larger in the inner disc, decreasing steeply outwardly. There is also a mutual anti-correlation between the index and SF coefficient, and the SF law can be expressed by a single-parameter function of the SF coefficient. The variable SF law is discussed in relation to self-regulation of SF.

Key words: H II regions – galaxies: individual (Milky Way) – ISM: molecular gas.

1 INTRODUCTION

The Schmidt–Kennicutt law (Schmidt 1959; Kennicutt 1998a,b), hereafter the star formation or SF law, has been extensively investigated in galaxies by measuring the surface densities of the star formation rate (SFR) and the surface or column gas densities projected on to the galactic planes (Schmidt 1959; Kennicutt 1998a,b; Komugi, Sofue & Egusa 2006; Bigiel et al. 2008; Leroy et al. 2008, 2013; Lada et al. 2012; Kennicutt & Evans 2012; and the large body of literature therein). It is established that the SF law represents the universal scaling relation in galactic-scale SF. Detailed analyses of the dependence of the law on the interstellar medium condition, particularly on the molecular gas, have been recently obtained in several galaxies, and the molecular-gas-regulated SF scenario has been proposed and modelled (Boissier et al. 2003; Booth, Theuns & Okamoto 2007; Leroy et al. 2008; Krumholz, McKee & Tumlinson 2009).

The SF law in the Milky Way has been investigated using individual star-forming regions associated with molecular and H I clouds and spiral arms (Fuchs et al. 2009; Luna et al. 2006; Heiderman et al. 2010; Willis et al. 2015; Heyer et al. 2016; and the papers cited therein). Recently, we analysed the Galactic distributions of H II regions, H_2, and H I gases to obtain a global SF law in the entire Milky Way with a spatial resolution of ∼1 kpc in the Galactic plane (Sofue & Nakanishi 2017, hereafter Paper I).

We showed that H II regions are distributed in a star-forming disc with a nearly constant full thickness of 92 pc in spatial coincidence with the molecular gas disc. With this thickness, the vertically averaged volume SFR, $\rho_{\rm SFR}$, was shown to be related to the surface SFR, $\Sigma_{\rm SFR}$, by $\rho_{\rm SFR}/[{\rm M}_\odot\,{\rm kpc}^{-3}\,{\rm yr}^{-1}] = \rho_{\rm SFR}/[{\rm M}_\odot\,{\rm pc}^{-3}\,{\rm Gyr}^{-1}] = 9.26\times\Sigma_{\rm SFR}/[{\rm M}_\odot\,{\rm yr}^{-1}\,{\rm kpc}^{-2}]$. This relation will be used throughout this paper.

In this paper, we examine the variations of both the volume and surface SF laws in the Galaxy. The volume SF law in the whole Galactic disc will be analysed in detail for the first time. It can be obtained uniquely by analysing the 3D data of H I and H_2 gas distributions. Both the volume and surface SF laws will be shown to be not universal in the Galaxy, but highly variable with the galactocentric distance and dependent on the SFR itself.

In the analyses, we use the H II region catalogue for the Milky Way (Hou & Han 2014) and the 3D maps of H I and H_2 gases (Nakanishi & Sofue 2003, 2006, 2016; Sofue & Nakanishi 2016), which were obtained by analysing the Leiden-Argentine-Bonn All Sky H I survey (Kalberla et al. 2005) and Galactic disc CO line survey (Dame, Hartman & Thaddeus 2001).

2 DEFINITION OF THE VOLUME AND SURFACE SFR AND THE DATA

Following the definition adopted in Paper I, we express the volume SFR by a power-law function of gas density, and represent it in logarithmic form as

$$\log\left(\frac{\rho_{\rm SFR}}{{\rm M}_\odot\,{\rm pc}^{-3}\,{\rm Gyr}^{-1}}\right) = \alpha\,\log\left(\frac{\rho_{\rm gas}}{{\rm H\,cm}^{-3}}\right) + A_{\rm vol}, \qquad (1)$$

where $\rho_{\rm SFR}$ is the vertically averaged volume SFR in the SF disc of full thickness 92 pc, and $A_{\rm vol} = A + 0.967$ with A being the coefficient between $\Sigma_{\rm SFR}$ and ρ as defined in Paper I. The coefficient $A_{\rm vol}$ represents the $\rho_{\rm SFR}$ at $\rho_{\rm gas} = 1\,{\rm H\,pc}^{-3}$. Similarly, the surface

* E-mail: sofue@ioa.s.u-tokyo.ac.jp

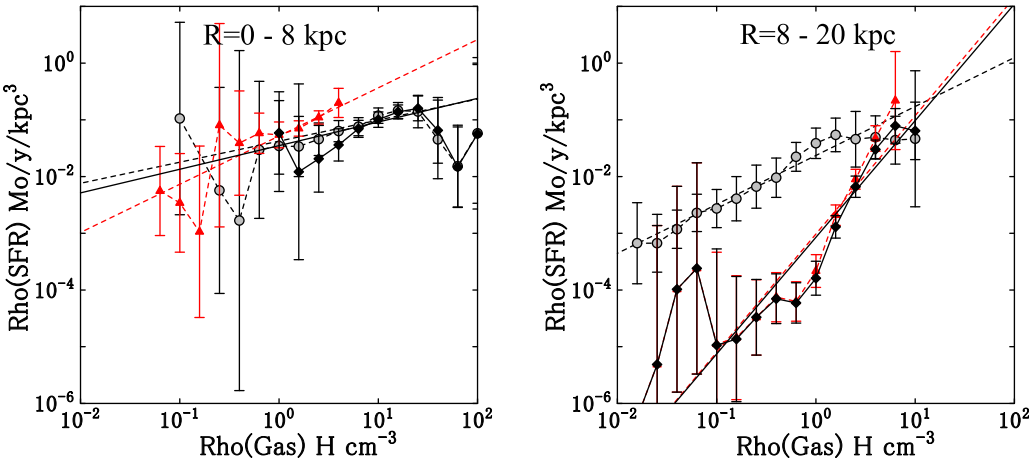

Figure 1. Inner ($R = 0$ to 8 kpc) and outer (8 to 20 kpc) volume SF laws in the Galaxy. Big grey circles are molecular gas, triangles are H I, and diamonds are the total (H I + H_2) gas. The straight lines are the least-squares fits to the plots. The unit for SFR is equivalent to $M_\odot$ pc^{-3} Gyr^{-1}.

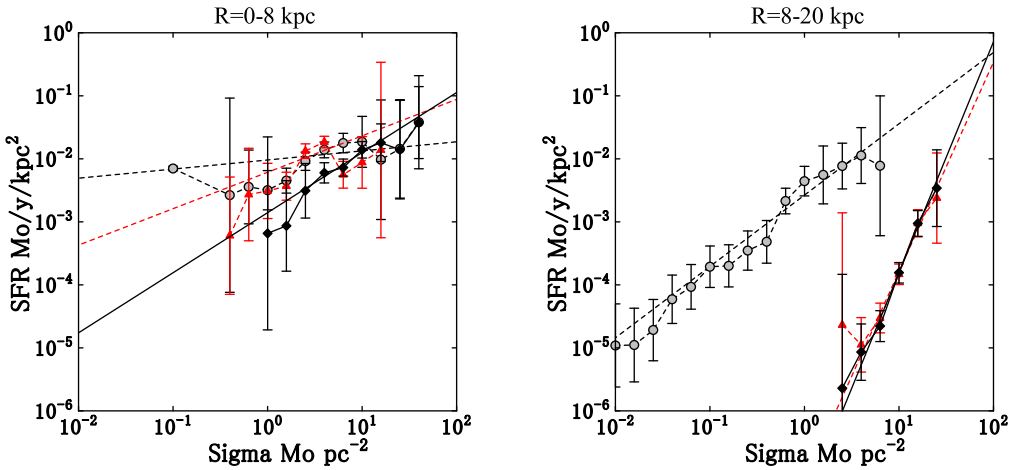

Figure 2. Same as Fig. 1, but for surface (integrated column) densities.

SFR law is expressed by

$$\log\left(\frac{\Sigma_{\rm SFR}}{\rm M_\odot\ yr^{-1}\ kpc^{-2}}\right) = \beta \log\left(\frac{\Sigma_{\rm gas}}{\rm M_\odot\ pc^{-2}}\right) + B, \qquad (2)$$

where the coefficient B represents $\Sigma_{\rm SFR}$ at $\Sigma_{\rm gas} = 1\,{\rm M_\odot\ pc^{-2}}$.

The SFR was calculated using the emission rates of UV photons of H II regions inferred from their excitation parameter from radio observations (Schraml & Mezger 1969; Hou & Han 2014). The incompleteness of the mapping of H II regions was corrected for by the detection probability, which is a function of the distance and intrinsic luminosity of each H II region. The distance errors are mostly kinematical distance errors due to the intrinsic velocity dispersion of H II regions, since recombination line velocity measurements had better resolution. They are of the same order as those for the H I and H_2 gases, ∼0.5 to 1 kpc, as described below. The number of effective independent data points in each plot of the SF law is the number of ∼1 × 1 kpc grids in the Galactic plane, which is taken into account when calculating the standard errors of the plotted quantities.

The SFR map was obtained by smoothing the UV emission rates by a Gaussian beam of full width at half-maximum 1 kpc (±0.5 kpc) in the Galactic plane. The vertical resolution depends on the telescope resolution and positioning, and was of the order of several arc minutes, or ∼7 pc for $\delta\theta \sim 5$ arcmin at ∼5 kpc distance, and was better than that for the gases, as discussed below. However, since the number of H II regions was not sufficient to divide the disc into a meaningful number of layers, we do not discuss the vertical variation.

The distribution maps of H I and H_2 gases in the Galaxy have a spatial resolution depending on their errors in kinematical distances and, therefore, on their distance from the Sun and their direction. Except for the velocity degenerate regions in the Galactic Centre and anti-Centre directions as well as along the solar circle, the distance error is about ∼0.5 to 1 kpc for an effective radial velocity uncertainty corresponding to the interstellar velocity dispersion of $\delta v_{\rm r} \sim 5$ km s^{-1} (see equation 23 of Sofue 2011), although the observational resolution of the LAB H I survey was 1.3 km s^{-1}.

3 RADIAL VARIATION OF STAR FORMATION LAW

We examined how the SF relation varies with the galacto-centric distance R. We obtained the same plots both for the volume and surface SF laws, and found the same or similar behaviours.

3.1 Non-universal SF law varying with radius

First, we divided the Galaxy into two areas, the inner disc at $R \leq$ 8 kpc and the outer disc at $R >$ 8 kpc, and derived the SF law in

Table 1. Index α and coefficient $A_{\rm vol}$ for volume SF law at different R ranges.

R (kpc)	α (Mol)	$A_{\rm vol}$ (Mol)	α (H I)	$A_{\rm vol}$ (H I)	α (Tot)	$A_{\rm vol}$ (Tot)
0.00–20.00	0.70 ± 0.07	−1.69 ± 0.07	2.29 ± 0.03	−2.59 ± 0.06	2.01 ± 0.02	−3.17 ± 0.04
0.00–8.00	0.37 ± 0.17	−1.38 ± 0.18	0.85 ± 0.27	−1.28 ± 0.10	0.42 ± 0.20	−1.45 ± 0.22
8.00–16.00	0.86 ± 0.14	−1.63 ± 0.11	2.09 ± 0.04	−3.00 ± 0.08	2.06 ± 0.04	−3.06 ± 0.07
0.00–2.00	0.61 ± 0.28	−2.40 ± 0.48	0.85 ± 0.41	−1.79 ± 0.26	0.43 ± 0.13	−2.07 ± 0.04
2.00–4.00	−0.73 ± 0.24	−0.56 ± 0.20	−0.72 ± 0.43	−1.10 ± 0.17	−0.80 ± 0.21	−0.41 ± 0.17
4.00–6.00	0.33 ± 0.19	−1.00 ± 0.20	0.52 ± 0.35	−0.82 ± 0.11	0.23 ± 0.10	−0.90 ± 0.09
6.00–8.00	0.41 ± 0.28	−1.40 ± 0.25	0.78 ± 0.53	−1.38 ± 0.18	0.55 ± 0.30	−1.60 ± 0.30
8.00–10.00	0.39 ± 0.20	−1.43 ± 0.11	2.85 ± 0.55	−2.55 ± 0.26	1.91 ± 0.50	−2.45 ± 0.29
10.00–12.00	0.42 ± 0.17	−2.31 ± 0.13	2.33 ± 0.58	−3.41 ± 0.24	1.85 ± 0.47	−3.35 ± 0.24
12.00–14.00	1.82 ± 0.68	−3.66 ± 0.20	1.83 ± 0.68	−3.66 ± 0.20	–	–
14.00–16.00	1.80 ± 0.20	−3.52 ± 0.40	1.91 ± 0.20	−3.30 ± 0.40	–	–
16.00–18.00	1.91 ± 0.20	−3.30 ± 0.40	–	–	–	–

Table 2. Index β and coefficient B for surface SF law at different R ranges.

R (kpc)	β (Mol)	B (Mol)	β (H I)	B (H I)	β (Tot)	B (Tot)
Galaxies[a]	–	–	–	–	1.4	−3.6
Milky Way						
0.00–20.00	1.10 ± 0.07	−2.57 ± 0.06	−1.13 ± 0.21	−2.25 ± 0.16	1.12 ± 0.37	−4.30 ± 0.36
0.00–8.00	0.14 ± 0.05	−2.02 ± 0.05	0.58 ± 0.31	−2.21 ± 0.17	0.95 ± 0.32	−2.85 ± 0.28
8.00–16.00	1.13 ± 0.11	−2.58 ± 0.11	3.13 ± 0.60	−6.91 ± 0.61	3.45 ± 0.59	−7.24 ± 0.60
0.00–2.00	1.43 ± 0.54	−3.82 ± 0.54	1.68 ± 0.90	−3.00 ± 0.32	1.61 ± 0.57	−4.14 ± 0.63
2.00–4.00	0.81 ± 0.73	−2.60 ± 0.36	1.00 ± 0.73	−2.42 ± 0.26	0.98 ± 0.86	−2.91 ± 0.61
4.00–6.00	0.50 ± 0.20	−1.94 ± 0.12	0.51 ± 0.27	−1.89 ± 0.13	1.04 ± 0.34	−2.55 ± 0.29
6.00–8.00	0.09 ± 0.07	−2.06 ± 0.07	−0.32 ± 0.47	−1.86 ± 0.30	0.39 ± 0.59	−2.49 ± 0.50
8.00–10.00	0.40 ± 0.22	−2.37 ± 0.12	0.69 ± 0.48	−3.12 ± 0.48	2.23 ± 0.69	−4.80 ± 0.74
10.00–12.00	0.66 ± 0.26	−3.14 ± 0.24	–	–	–	–
12.00–14.00	1.00 ± 0.33	−3.03 ± 0.49	–	–	–	–
14.00–16.00	−1.23 ± 0.42	−7.90 ± 0.81	–	–	–	–

Note. [a]Kennicutt (1998a).

each area. Figs 1 and 2 show the results, where the straight lines are the least-squares fitting to the plots in the log–log plane. Tables 1 and 2 list the best-fitting values for the indices and coefficients. In the first row of the tables, we list the parameters obtained in Paper I for the whole Galaxy for comparison.

There is a remarkable difference in the SF laws in the inner and outer discs. The inner SF law has a significantly smaller power-law index compared to that in the outer disc. Also, the average value of the SFR is greater in the inner disc, trivially reflecting that SF activity is higher in the inner disc because of the higher gas density.

To examine finer variations with R, we further divided the Galaxy into a larger number of rings of 2 kpc width. The volume and surface SF laws for individual rings are shown in the Appendix in Figs A1 and A2, respectively. We fitted each plot by least-squares fitting, and show the result with straight lines. The best-fit values are listed in Tables 1 and 2.

There are shorter-scale variations of the SF law with the radius. Besides the generally flat index in the inner Galaxy, the flattest or even an inverse index of the volume SF law was found at $R = 2$–4 kpc. On the other hand, the surface SF law exhibits the flattest index at $R = 4$–6 kpc, and the innermost and Galactic Centre regions have again a steep index.

The inverse volume SF law at $R = 2$–4 kpc indicates that the SFR decreases with increasing gas density. This apparently strange behaviour could be understood if some regulation mechanism is working in such a way that SF is strongly suppressed when the SFR exceeds a certain threshold value. In the present case, this threshold exists at $\rho_{\rm SFR} \sim 0.1\,{\rm M}_\odot\,{\rm pc}^{-3}\,{\rm Gyr}^{-1}$. It must be also emphasized that the region coincides in position with the 4-kpc molecular ring with the highest SFR in the Galaxy.

Another remarkable nature of the SF laws at $R \lesssim 8$ kpc is the coincidence of both the index and coefficient for H_2 with those for H I and total gases. This may reflect that the inner Galactic disc is dominated by molecular gas and that the H I gas density is saturated at a threshold density related to the molecular gas density (Sofue & Nakanishi 2016).

In contrast, the SF law for H_2 gas in the outer Galaxy at $R \gtrsim 8$ kpc is significantly displaced from those for H I and total gases, which have a much milder index. Also, the outer SF laws are like that obtained in the entire Galactic disc in Paper I. This means that the global SF law is determined more by the laws in the outer Galaxy for the larger area, and hence, there is a larger weight in the averaging.

Thus, the global SF law, often regarded as the universal scaling relation, reflects more the SF relations in the outer disc. This sounds paradoxical in the sense that the universal SF law may not necessarily be a direct measure of the most active SF in the galaxy. Namely, the most active SF in the galaxy cannot be investigated by an analysis of the global SF law.

This paradox reminds us of the SF law in starburst galaxies, which is significantly displaced from the universal SF law for normal galaxies (Komugi et al. 2005, 2006). This displacement could be

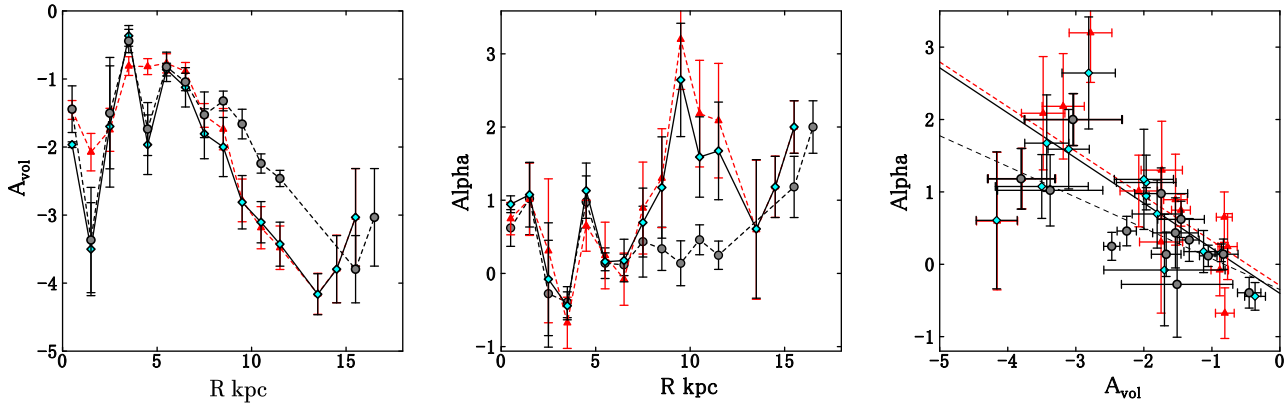

Figure 3. Left: Radial variation of $A_{\rm vol}$. Middle: Same for α. Right: Correlation between α and $A_{\rm vol}$. Lines show the least-squares fits to individual plots (dash for H_2, thin dash for H I and solid for total). Symbols are as before.

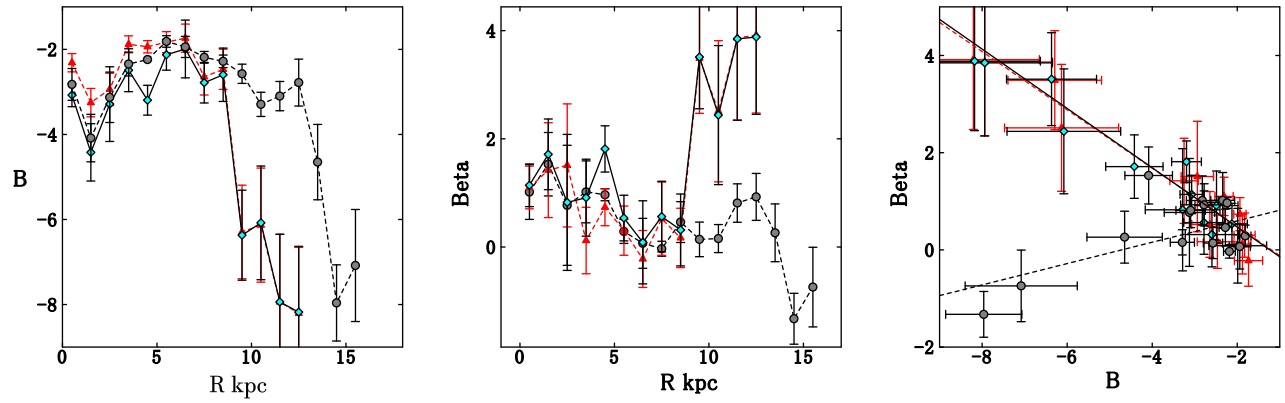

Figure 4. Same as Fig. 3, but for surface relations.

due to selectively observed active SF regions in starbursts, which have intrinsically larger SF coefficients.

3.2 Variable SF coefficients and indices

In Figs 3 and 4, we show the SF coefficients and power-law indices as a function of the radius R, as obtained by the least-squares fitting to the SF law plots at 1 kpc radius interval. We also show the relation between the index and coefficient.

The $A_{\rm vol}$ versus R and B versus R relations demonstrate and confirm that the SFR varies with the radius, revealing higher SFR in the inner region and the steep decrease towards the outer Galaxy. This decrease obviously follows the decrease of the gas density with the radius.

The $A_{\rm vol}$ versus R and B versus R relations show that the SF power-law index for molecular gas remains nearly constant within $R \lesssim 8$ kpc. The index for H_2 gas in the volume SF law, then, increases towards the outer region. In contrast, the H_2 index for the surface law seems to remain constant or even decreases. On the other hand, the indices for volume and surface H I and total gases show similar behaviours, increasing towards the observed outer edge.

An interesting finding in these plots is that the SF parameters, $A_{\rm vol}$, α, B and β, are not constant at all, showing that the SF law in the Galaxy is not universal. The values of $A_{\rm vol}$ and B vary over three orders of magnitudes from the inner to the outer Galaxy. This variable SF law may contradict the currently established universal SF law in galaxies, which requires a constant value of the coefficients $A_{\rm vol}$ and B for a given value of gas density.

In Fig. 5, we plot the fitted coefficients and indices for the volume and surface SF laws used in Figs 3 and 4. The plotted values are not perfectly independent because the $\rho_{\rm SFR}$ and $\Sigma_{\rm SFR}$ used are linearly related. Therefore, these plots include the correlation between the volume and surface gas densities used. It is readily shown that the SF coefficients $A_{\rm vol}$ and B are linearly correlated at high SF regions showing $A_{\rm vol} = B + 0.967$ by the definition of volume and surface SFR, except for low SF regions corresponding to the low-density outer Galaxy. The power-law indices are weakly correlated to each other as $\beta \sim 1.63\alpha$, and are largely scattered around this relation.

Besides the radial variation, there exists a mutual correlation between the power-law index and SF coefficient, as shown in Figs 3 and 4. The plots reveal a clear anti-correlation between the index and coefficient. This implies that the SF law is controlled also by SFR in the sense that the higher the SFR, the flatter is the index.

If the correlation can be represented by relations like

$$\alpha = \alpha_0 + cA_{\rm vol} \tag{3}$$

and

$$\beta = \beta_0 + dB, \tag{4}$$

we obtain the values listed in Table 3. Inserting these parameters in equations (1) and (2), we have empirical SF laws with a single-parameter function. This formulation may become a generalization of the current SF law, which had two parameters for the index (α or β) and SF coefficient ($A_{\rm vol}$ or B).

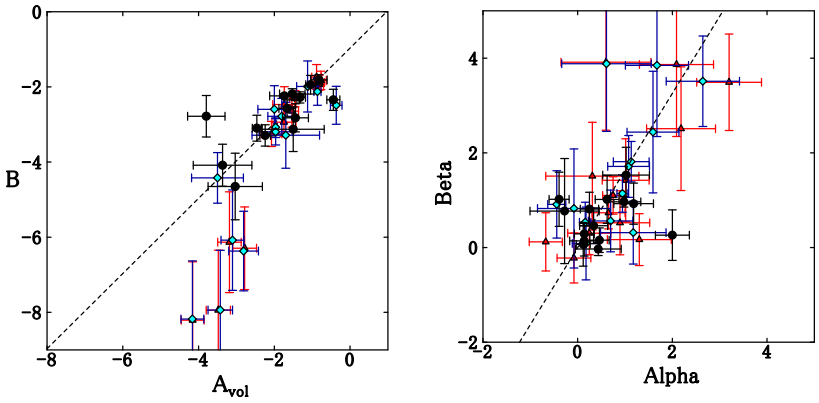

Figure 5. Correlation between fitted SF coefficients of surface and volume SF laws used in Figs 3 and 4 (left), and the same between power-law indices (right). Circles, triangles and diamonds denote H_2, H I and total gases, respectively.

Table 3. Empirical relations between the index and coefficient.

Index	Coefficient
$\alpha_{0:\mathrm{mol}} = -0.35 \pm 0.15$	$c_{\mathrm{mol}} = -0.42 \pm 0.08$
$\alpha_{0:\mathrm{HI}} = -0.29 \pm 0.22$	$c_{\mathrm{H\,I}} = -0.62 \pm 0.11$
$\alpha_{0:\mathrm{tot}} = -0.40 \pm 0.15$	$c_{\mathrm{tot}} = -0.62 \pm 0.07$
$\beta_{0:\mathrm{mol}} = 1.04 \pm 0.18$	$d_{\mathrm{mol}} = +0.22 \pm 0.07$
$\beta_{0:\mathrm{HI}} = -0.72 \pm 0.36$	$d_{\mathrm{H\,I}} = -0.60 \pm 0.13$
$\beta_{0:\mathrm{tot}} = -0.75 \pm 0.47$	$d_{\mathrm{tot}} = -0.61 \pm 0.14$

3.3 Self-regulation of SF

The highest A_{vol} and B, and hence the most active SF activity, is found in a radial zone at $R \sim 3$–6 kpc centred by the 4-kpc molecular ring (Figs 3 and 4). The corresponding Schmidt plots in the panels at $R = 2$–6 kpc of Figs A1 and A2 exhibit flat slopes with indices less than 1.

Such a flat SF law may imply that SF in high-SFR regions tends to be saturated by molecular gas dissociation due to UV emission as well as by injection of kinetic and thermal energy by stellar winds and supernova explosions in active SF regions (Krumholz et al. 2009).

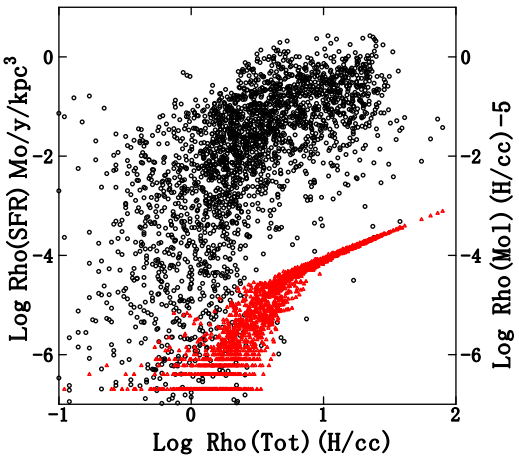

Figure 6. Schmidt plot of SFR against ρ_{tot} (raw data from Paper I: grey circles). Triangles show H_2 gas density ($\rho_{H_2} \times 10^{-5}$) plotted against ρ_{tot}, showing the phase transition from H I to H_2 around the threshold density of $\rho_{\mathrm{tot}} \sim 3$ H cm^{-3}. The bend from steep to mild index occurs around this threshold density.

4 SUMMARY AND DISCUSSION

The Schmidt–Kennicutt law between the volume SFR ρ_{SFR} and volume gas densities ρ_{gas} of H I, H_2 and total gases was shown to vary with the galacto-centric distance R. It was shown that the SF power-law index α is significantly smaller in the inner disc than in the outer Galaxy. Even an inverse index was found at radii near the 4-kpc molecular ring. The SF index was also found to be inversely correlated with the coefficient A_{vol} of SFR, suggesting regulation of SFR by increasing SF activity. Similar results were obtained also for the surface SF laws. We, thus, suggest that the resolved SF law in the Galaxy may be not be uniform nor does it give the universal scaling relation.

Variation of the SF index depending on the gaseous phase may be explained by molecular-gas-regulated SF (e.g. Krumhotz et al. 2009). If we assume that molecular clouds are formed from H I gas by a power law such as $\rho_{H_2} \propto \rho_{\mathrm{H\,I}}^n$, we may expect that $\alpha(\mathrm{H\,I}) \sim \alpha(H_2) + n > \alpha(H_2)$, and similarly for β. The variable SF index may be, thus, a measure of the directness of SF in the sense that the more the additional process is involved prior to SF, the steeper is the index. This may also explain the steeper index of SF laws for surface gas densities than for volume densities. In other words, the α index is a more direct measure of SF than β, trivially indicating that SF is more directly related to the volume density than to the column density.

This consideration may also apply to the SF law for total gas, for which the index is a mixture of indices for H_2 and H I, and is steeper than the index for H_2 gas. It was also found in Paper I that the SF power-law index for total gas has a bend from steep to milder around the threshold density of $\rho_{\mathrm{tot}} \sim 3$ H cm^{-3}, which we reproduce in Fig. 6. In the figure, we compare this SF law with the plot of molecular gas density against the total gas density, where also a bend exists. Both the bends appear at the same threshold density of $\rho_{\mathrm{tot}} \sim 3$ H cm^{-3}. These bent behaviours are in agreement with the model of molecular-gas-regulated SF in galaxies (Booth et al. 2007; Bigiel et al. 2008), and the bent SF law readily found in galaxies (Krumholz et al. 2009).

The H I-to-H_2 transition in low-density regions, where SF is settled from forming H_2 gas, makes the SF index steeper than that in the molecular-gas-dominant regions. The steeper index in the outer Galaxy with lower density and lower molecular fraction reflects such indirect SF, where the index tends to become larger because

of the additional processes of transition from H I to H_2 and the formation of molecular clouds.

The ρ_{SFR} versus ρ_{H_2} law is, thus, considered to be a direct measure of SF (Krumhotz et al. 2009). The other relations for $\rho_{H\,I}$, ρ_{tot}, $\Sigma_{H\,I}$ and Σ_{tot} must be analysed more carefully by taking into account the intervening processes, such as the phase transition between H_2 and H I, and the formation and dissociation of molecular clouds. The current studies used the surface relations, which implicitly contain the indirect or unrelated H I gas by projecting it on to the Galactic plane.

ACKNOWLEDGEMENTS

The author thanks Dr H. Nakanishi of Kagoshima University for the H I and H_2 3D cube data.

REFERENCES

Bigiel F., Leroy A., Walter F., Brinks E., de Blok W. J. G., Madore B., Thornley M. D., 2008, AJ, 136, 2846
Boissier S., Prantzos N., Boselli A., Gavazzi G., 2003, MNRAS, 346, 1215
Booth C. M., Theuns T., Okamoto T., 2007, MNRAS, 376, 1588
Dame T. M., Hartman D., Thaddeus P., 2001, ApJ, 547, 792
Fuchs B., Jahreis H., Flynn C., 2009, AJ, 137, 266
Heiderman A., Evans N. J., II, Allen L. E., Huard T., Heyer M., 2010, ApJ, 723, 1019
Heyer M., Gutermuth R., Urquhart J. S., Csengeri T., Wienen M., Leurini S., Menten K., Wyrowski F., 2016, AA, 588, A29
Hou L. G., Han J. L., 2014, A&A, 569, A125
Kalberla P. M. W., Burton W. B., Hartmann D., Arnal E. M., Bajaja E., Morras R., Pöppel W. G. L., 2005, AA, 440, 775
Kennicutt R. C., 1998a, ApJ, 498, 541
Kennicutt R. C., 1998b, ARAA, 36, 189
Kennicutt R. C., Evans N. J., 2012, ARAA, 50, 531
Komugi S., Sofue Y., Nakanishi H., Onodera S., Egusa F., 2005, PASJ, 57, 733
Komugi S., Sofue Y., Egusa F., 2006, PASJ, 58, 793
Krumhotz M. R., McKee C. F., Tumlinson J., 2009, ApJ, 693, 235
Lada C. J., Forbrich J., Lombardi M., Alves J. F., 2012, ApJ, 745, 190
Leroy A. K., Walter F., Brinks E., Bigiel F., de Blok W. J. G., Madore B., Thornley M. D., 2008, AJ, 136, 2782
Leroy A. K. et al., 2013, AJ, 146, 19
Luna A., Bronfman L., Carrasco L., May J., 2006, ApJ, 641, 938
Nakanishi H., Sofue Y., 2003, PASJ, 55, 191
Nakanishi H., Sofue Y., 2006, PASJ, 58, 847
Nakanishi H., Sofue Y., 2016, PASJ, 68, 5
Schmidt M., 1959, ApJ, 129, 243
Schraml J., Mezger P. G., 1969, ApJ, 156, 269
Sofue Y., 2011, PASJ, 63, 813
Sofue Y., Nakanishi H., 2016, PASJ, 68, 63
Sofue Y., Nakanishi H., 2017, PASJ, 69, 19 (Paper I)
Willis S., Guzman A., Marengo M., Smith H. A., Martínez-Galarza J. R., Allen L., 2015, ApJ, 809, 87

APPENDIX A: VOLUME AND SURFACE SF LAWS IN ANNULUS RINGS

In this appendix, we show in Fig. A1 volume SF laws (plots of ρ_{SFR} against ρ_{gas}) for individual annular rings of 2 kpc width, and in Fig. A2 surface SF laws (Σ_{SFR} against Σ_{gas}). The lines show the least-squares fitting results, and the parameters (indices and coefficients) are listed in Tables 1 and 2.

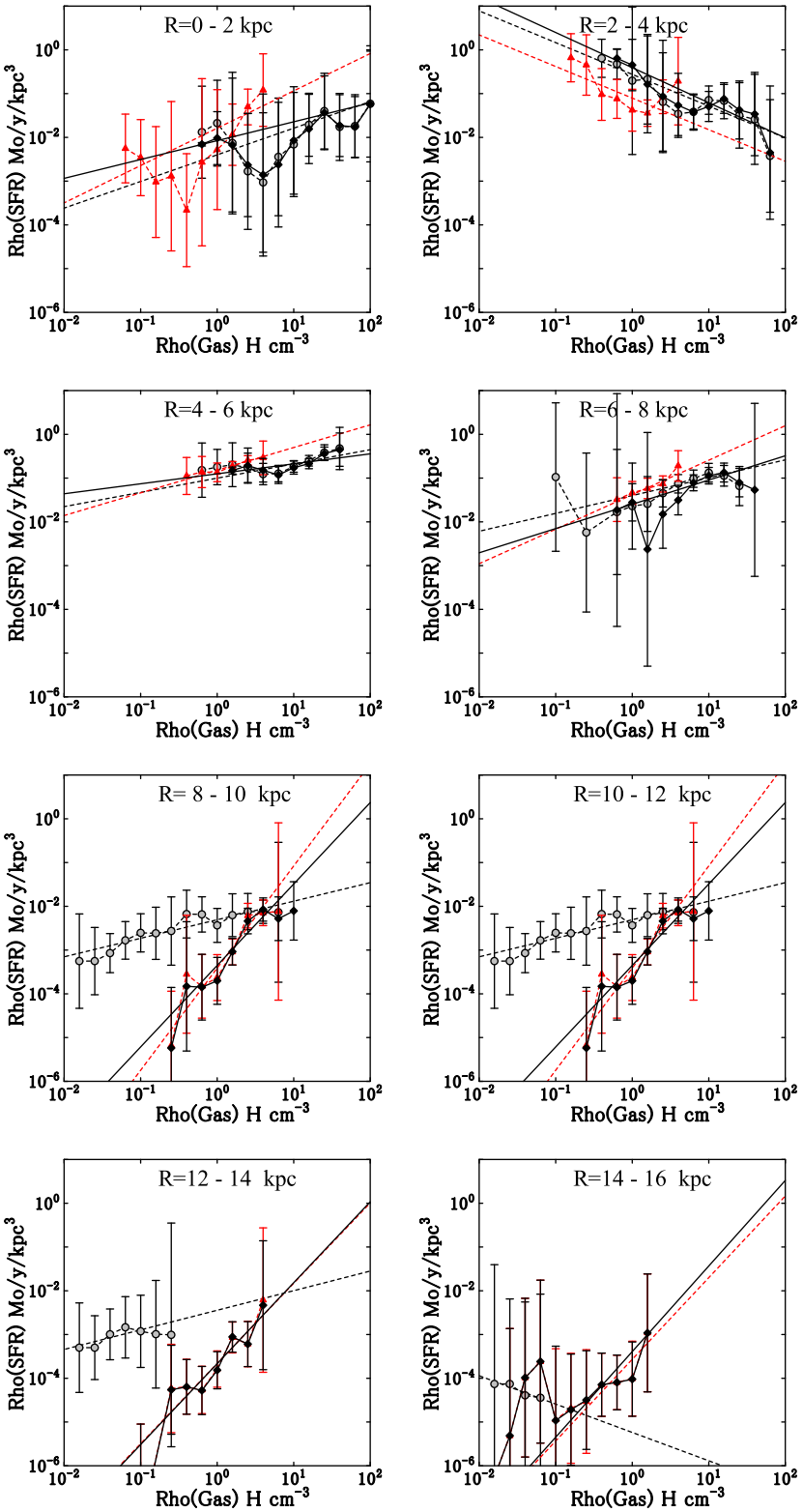

Figure A1. Radial variation of volume SF law at different radii plotted at 2-kpc intervals. Circles, triangles and diamonds denote $\rho_{\rm SFR}$ for volume densities of H_2, H I and total gases, respectively.

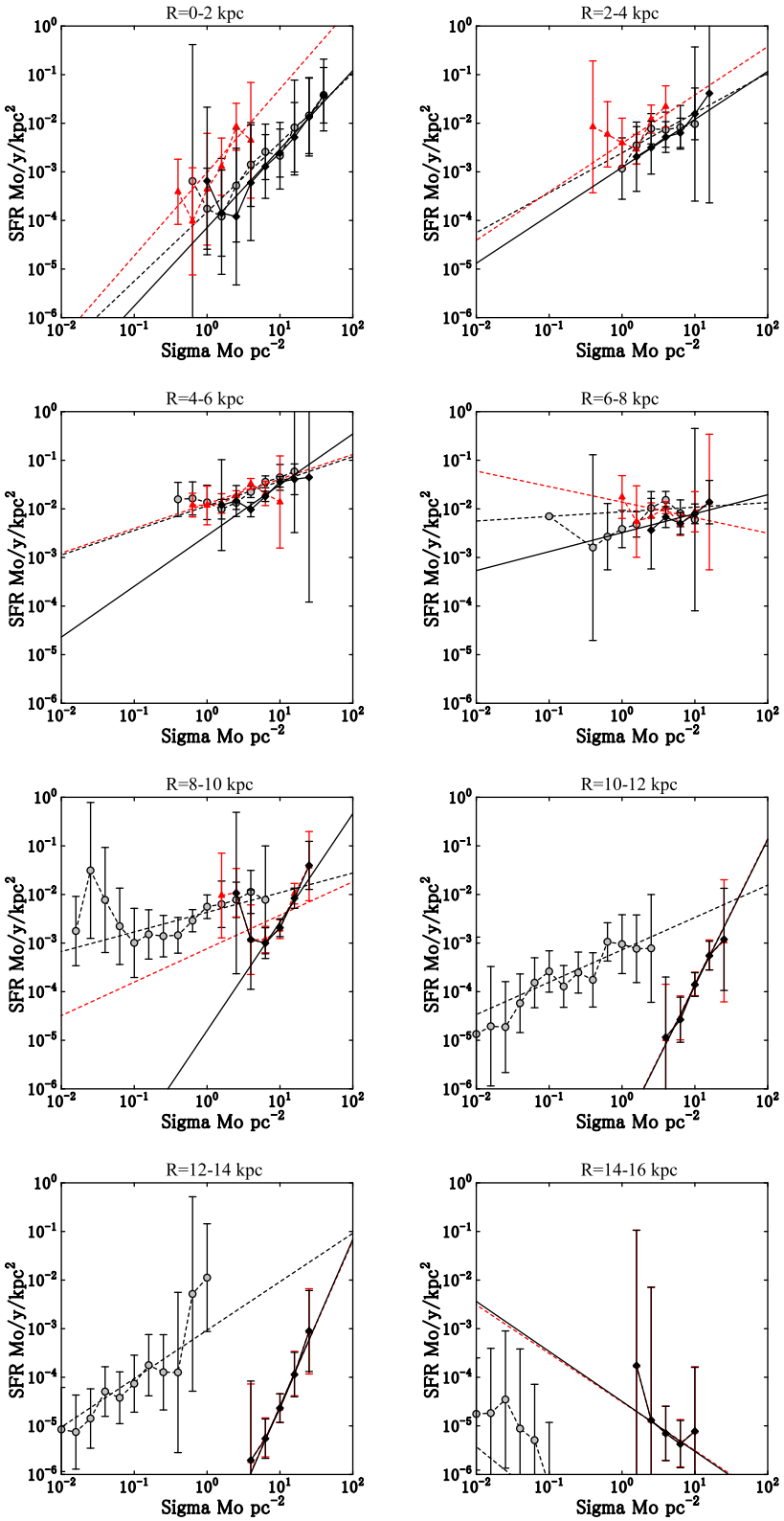

Figure A2. Same as Fig. A1, but for the surface SFR. Circles, triangles and diamonds denote Σ_{SFR} for surface densities of H_2, H I and total gases, respectively.

This paper has been typeset from a TEX/LATEX file prepared by the author.